Performance Analysis of Optimally Coordinated Connected and Automated Vehicles in a Mixed Traffic Environment

Alejandra Valencia, *Student Member, IEEE*, A M Ishtiaque Mahbub, *Student Member, IEEE*, Andreas A. Malikopoulos, *Senior Member, IEEE*

***Abstract*— Trajectory planning of connected and automated vehicles (CAVs) poses significant challenges in a mixed traffic environment due to the presence of human-driven vehicles (HDVs). In this paper, we apply a framework that allows optimal coordination of CAVs and HDVs traveling through a traffic corridor consisting of an on-ramp merging, a speed reduction zone, and a roundabout. We study the impact of different penetration rates of CAVs and traffic volumes on the efficiency of the corridor. We provide extensive simulation results and report on the benefits in terms of total travel time and fuel economy.**

I. Introduction

The emergence of connected and automated vehicles (CAVs) enables a novel computational framework to provide real-time control actions that optimize energy consumption and associated benefits such as improving travel time and significantly reducing stop-and-go driving. By optimally controlling CAVs, we can alleviate congestion at different traffic scenarios, reduce emission, improve fuel efficiency and increase passenger safety [1]–[4]. Several efforts in the literature have addressed the problem of optimal coordination of CAVs to improve the vehicle- and network-level performances [5]–[10]. Recent efforts have reported results on coordination of CAVs at on-ramp merging roadways, roundabouts, speed reduction zones, signal-free intersections, and traffic corridors (see [11]–[16]).

It is expected that CAVs will gradually penetrate the market and interact with human-driven vehicles (HDVs) by 2060 [17]. However, different penetration rates of CAVs can significantly alter transportation efficiency and safety. While the aforementioned studies have shown the benefits of CAVs to reduce energy and alleviate traffic congestion in specific traffic scenarios, most of these efforts have focused on 100% CAV penetration rates without considering HDVs.

One of the research directions towards controlling the CAVs in a mixed traffic environment has been the development of adaptive cruise control [18]–[20] where a CAV, preceded by a single or a group of HDVs, applies cruise control to optimize a given objective, e.g., improvement of fuel economy [21], minimization of backward propagating wave [22], [23], etc. Although these research efforts [24] aim at enhancing our understanding of improving the efficiency through coordination of CAVs in a mixed traffic environment, deriving a tractable solution to the problem of CAV coordination at merging or roundabout scenario still remains challenging. Several approaches reported in the literature implemented well-known car-following models, which emulate the human-driving behavior [25], [26], to derive a deterministic quantification of the vehicle trajectory [27], [28]. Other approaches have used car-following models [29] or learning algorithms [30], [31] for CAV coordination in mixed traffic environment. There have been also some research efforts that have investigated the effects of CAV penetration on a mixed traffic network through microscopic [32] or meso/macroscopic simulation [33], [34] environments.

In this paper, we analyze the impact of optimally coordinating CAVs traveling through a mixed traffic corridor including three different scenario: on-ramp merging, speed reduction zone and roundabout. In this context, CAVs interact with HDVs at varying penetration rates and different traffic volumes. The contributions of this paper are the (i) development of a simulation environment of an optimal CAV coordination framework at a corridor in a mixed traffic network, and (ii) a detailed analysis of the impact of CAV penetration on the vehicle- and network level performance, in terms of fuel economy and travel time, under different traffic volumes.

The remainder of the paper proceeds as follows. In Section II, we provide the modeling framework for a mixed traffic environment. In Section III, we present the coordination framework for CAVs traveling through the traffic corridor while interacting with HDVs. In Section IV, we provide a detailed analysis and simulation results. Finally, we draw concluding remarks in Section V.

II. Problem Formulation

We consider the University of Michigan's Mcity where CAVs and HDVs are traveling through a particular test route as illustrated by the black trajectory in Fig. 1. The route consists of three traffic scenarios, indexed by $z = 1, 2, 3$, representing a highway on-ramp, a speed reduction zone, and a roundabout, respectively. Note that to create traffic congestion in the test route, we consider additional traffic flow at the adjacent roads.

Upstream of each traffic scenario, we define a *control zone* where CAVs coordinate with each other to avoid any rear-end or lateral collision. The length of the control zone is $L_z \in \mathbb{R}^+$ for each traffic scenario z. Since the

This research was supported by ARPAE's NEXTCAR program under the award number DE-AR0000796.

The authors are with the Department of Mechanical Engineering, University of Delaware, Newark, DE 19716 USA (emails: aleval@udel.edu; mahbub@udel.edu; andreas@udel.edu.)

Fig. 1: Corridor of Mcity with three traffic scenarios: on-ramp merging, speed reduction zone and roundabout.

HDVs do not share their state information, we consider the presence of *coordinators*, which can be loop-detectors, roadside units, or comparable sensory devices, that collect the state information of the HDVs traveling within each control zone. The coordinators transmit the HDVs' state information to each CAV within each control zone using standard vehicle-to-infrastructure communication protocols. Note that, the coordinators do not make any control decisions for the CAVs. They only handle the information flow for the CAVs and HDVs within each control zone. We define the area of potential lateral collision to be the *merging zone* of length S_z specific to traffic scenario z, as illustrated by the red marked area numbers 1, 2, and 3 in Fig. 1. The objective of each CAV is to derive its optimal control input (acceleration/deceleration) to cross the traffic scenarios without any rear-end or lateral collision with the other CAVs and HDVs.

Let $t_i^{0,z}$ be the time when each vehicle i enters the control zone towards traffic scenario z, $t_i^{m,z}$ be the time when the each vehicle enters the merging zone of the traffic scenario z, and $t_i^{f,z}$ be the time when vehicle i exits the corresponding merging zone. Let $\mathcal{N}_z = \{1, \dots, N(t)\}$, $t \in \mathbb{R}^+$, be a queue of vehicles to be analyzed for traffic scenario z, where $N(t)$ is the total number of CAVs within the control zone of the specific traffic scenario z at time $t \in \mathbb{R}^+$. We denote $\mathcal{N}_{\text{cav}}$ and $\mathcal{N}_{\text{hdv}}$ to be the set of CAVs and HDVs such that $\mathcal{N}_{\text{cav}} \cup \mathcal{N}_{\text{hdv}} = \mathcal{N}_z$.

The dynamics of each vehicle $i \in \mathcal{N}_z$, are represented as

$$\dot{\mathbf{x}}(t) = f(\mathbf{x}_i, u_i), \;\; \mathbf{x}_i(t_i^{0,z}) = \mathbf{x}_i^{0,z}, \tag{1}$$

where $\mathbf{x}_i(t), u_i(t)$ are the state and control input, respectively. For simplicity, we model each vehicle as a double integrator, i.e., $\dot{p}_i = v_i(t)$ and $\dot{v}_i = u_i(t)$, where $p_i(t) \in \mathcal{P}_i, v_i(t) \in \mathcal{V}_i$, and $u_i(t) \in \mathcal{U}_i$ denote the position, speed, and acceleration/deceleration (control input) of each vehicle i. Let $\mathbf{x}_i(t) = [p_i(t) \; v_i(t)]^T$ denote the state of each vehicle i, with initial value $\mathbf{x}_i(t_i^{0,z}) = [p_i(t_i^{0,z}) \; v_i(t_i^{0,z})]^T$.

In our modeling framework, we impose the following state and control constraints,

$$\begin{aligned} u_{\min} \le u_i(t) \le u_{\max}, \;\; &\text{and} \\ 0 \le v_{\min} \le v_i(t) \le v_{\max}, \;\; &\forall t \in [t_i^{0,z}, \; t_i^{f,z}], \end{aligned} \tag{2}$$

where $u_{\min}, u_{\max}$ are the minimum deceleration and maximum acceleration, $v_{\min}, v_{\max}$ are the minimum and maximum speed limits respectively. Next, we consider the rear-end and lateral safety constraints as

$$s_i(t) = p_k(t) - p_i(t) \ge \delta_i(t), \;\; \forall t \in [t_i^{0,z}, \; t_i^{f,z}], \tag{3}$$

where vehicle k is immediately ahead of i on the same lane. Lateral collision between any two vehicles $i, j \in \mathcal{N}_z$ can be avoided if the following constraint holds

$$\Gamma_i \cap \Gamma_j = \varnothing, \;\; \forall t \in [t_i^{m,z}, t_i^{f,z}], \quad i, j \in \mathcal{N}_z(t), \tag{4}$$

where $\Gamma_i := \{t \mid t \in [t_i^{m,z}, t_i^{f,z}]\}$.

For the CAV $i \in \mathcal{N}_{\text{cav}}$, the control input $u_i(t)$ in (1) can be derived within the control zone, the structure of which we discuss in Section III. In contrast, we consider a generic car-following model of the following form to derive the control input of each HDV $i \in \mathcal{N}_{hdv}$,

$$u_i(t) = f(p_i(t), p_{i-1}(t), v_i(t), v_{i-1}(t)), \tag{5}$$

where the function f represents the behavioral model of the car-following dynamics. In this paper, we employ the Wiedemann car-following model proposed in [26].

In the modelling framework presented above, we impose the following assumptions.

Assumption 1. The communication among the CAVs and the coordinator occurs without any transmission latency, errors or data loss.

Assumption 2. No lane change is allowed inside the control zone.

Assumption 1 might be strong, but can be relaxed as long as the noise in the measurements and/or delays is bounded. Assumption 2 simplifies the formulation by restricting the traffic flow to a single lane within the control zone.

III. Optimal Coordination Framework

For each CAV $i \in \mathcal{N}_{\text{cav}}$, we adopt the optimal control problem presented in [35], i.e.,

$$\min_{u_i} \frac{1}{2} \int_{t_i^{0,z}}^{t_i^{m,z}} u_i^2(t) dt, \;\; \forall i \in \mathcal{N}_z, \;\; \forall z = 1, 2, 3, \tag{6}$$

$$\text{subject to : } (1), (2),$$

$$p_i(t_i^{0,z}) = p_i^{0,z}, \; v_i(t_i^{0,z}) = v_i^{0,z}, \; p_i(t_i^{m,z}) = p_z,$$

$$\text{and given } t_i^{0,z}, \; t_i^{m,z},$$

where p_z is the location (i.e., entry position) of merging zone z; $p_i^{0,z}$, $v_i^{0,z}$ are the initial position and speed of vehicle i when it enters the control zone of traffic scenario z, respectively. The merging time $t_i^{m,z}$ can be obtained by

solving an upper-level control problem including the safety constraints (3), (4) in an iterative manner, as detailed in [35]. Suppose that, each CAV $i \in \mathcal{N}_z$ is aware of the information of the sets $\mathcal{L}_i^z$ and $\mathcal{C}_i^z$, which contain the unique id of the preceding vehicles travelling on the same lane, or on a conflict lane relative to CAV i, respectively. Then, each CAV i determines the time $t_i^{m,z}$ that will be entering the traffic zone $z = 1, 2, 3$, upon arrival at the entry of the corridor as follows (see [35]). If vehicle $(i-1) \in \mathcal{L}_i^z$ and $(i-1) \in \mathcal{N}_{\text{cav}}$, we have

$$t_i^{m,z} = \max\left\{ \min\left\{ t_{i-1}^{m,z} + \frac{\delta(v_i(t))}{v_{i-1}(t_{i-1}^{m,z})}, t_i^{0,z} + \frac{L_z}{v_{\min}} \right\}, t_i^{0,z} + \frac{L_z}{v_0(t_i^{0,z})}, t_i^{0,z} + \frac{L_z}{v_{\max}} \right\}, \tag{7}$$

while, if vehicle $(i-1) \in \mathcal{C}_i^z$ and $(i-1) \in \mathcal{N}_{\text{cav}}$, then

$$t_i^{m,z} = \max\left\{ \min\left\{ t_{i-1}^{m,z} + \frac{S_z}{v_{i-1}(t_{i-1}^{m,z})}, t_i^{0,z} + \frac{L_z}{v_{\min}} \right\}, t_i^{0,z} + \frac{L_z}{v_0(t_i^{0,z})}, t_i^{0,z} + \frac{L_z}{v_{\max}} \right\}, \tag{8}$$

where L_z and S_z are the length of the control zone and the length of the area of potential lateral collision, respectively.

Note that, if the vehicle preceding CAV i is an HDV, i.e., $(i-1) \in \mathcal{N}_{\text{hdv}}$, then we apply $t_{i-1}^{m,z} = t_{i-1}^{0,z} + \frac{L_z}{v_{i-1}(t_{i-1}^{0,z})}$ to estimate the merging time $t_{i-1}^{m,z}$ of HDV $i-1$. We then use $t_{i-1}^{m,z}$ in (7)-(8) to derive the merging time $t_i^{m,z}$ of CAV i. The recursion of the above computation is initialized when the first vehicle enters the control zone.

Using Hamiltonian analysis [36], the unconstrained optimal control input $u_i^*(t)$ of CAV $i \in \mathcal{N}_z$ and the corresponding state trajectories at time $t \in [t_i^{0,z},\ t_i^{m,z}]$ are [37]

$$u_i^*(t) = a_i \cdot t + b_i, \tag{9}$$

$$v_i^*(t) = \frac{1}{2} a_i \cdot t^2 + b_i \cdot t + c_i, \tag{10}$$

$$p_i^*(t) = \frac{1}{6} a_i \cdot t^3 + \frac{1}{2} b_i \cdot t^2 + c_i \cdot t + d_i, \tag{11}$$

where a_i, b_i, c_i, and d_i are the constants of integration and can be computed using the analysis presented in [37].

For the control of CAVs in a mixed environment, if the physically leading vehicle of a CAV is HDV, the CAV will probe the safety constraint continuously to make adjustment to its travel behavior. A switching mechanism is applied in the study: the control algorithm for a CAV would always be switched on until the safety constraint (3) is activated in terms of the distance between itself and its preceding HDV.

IV. Simulation and Discussion

A. Simulation Setup

To implement the control framework presented in the previous section, we use the microscopic multi-modal commercial traffic simulation software PTV VISSIM [38], [39] by creating a simulation environment replicating Mcity, as shown in Fig. 1. The corridor through which the vehicle travels has a length of 1,300 m within the Mcity. The maximum and minimum acceleration considered for each vehicle are 1.5 m/s^2 and -3.0 m/s^2, respectively. The speed limit on the on-ramp merging, speed reduction zone and roundabout are 40 m/s, 18.6 m/s and 25 m/s, respectively. The control zone length is 150 m and safe headway time considered is 1.2 s.

In our study, we consider the following three different cases:

Baseline: We construct the baseline case considering all the vehicles to be HDVs and without any communication capability. The vehicles subscribe to the VISSIM built-in Wiedemann car following model [26] to emulate the driving behavior of real human driven vehicles. We adopt priority based (yield/stop) traffic movement at the roundabout and on-ramp merging scenarios.

Optimal Coordination: In this case, all the vehicles are CAVs, and communicate with each other inside the control zone. Therefore, they can optimize their individual travel time and fuel efficiency, and plan their optimal trajectories. We consider three isolated coordinators for each traffic scenario. For the uncontrolled paths in-between the control zones, the CAVs revert back to the Wiedemann car following model [26] to traverse their respective routes. To apply the optimal control framework, we override VISSIM's built-in car following module and associated attributes using the DriverModel API.

Partial Penetration: To simulate the partial penetration case, we consider both of the above cases as the two extremes, and traverse the cases in between with different percentage of CAV inclusion. We adopt a priority based (yield/stop) traffic movement at the roundabout and on-ramp merging scenarios only for the HDVs, whereas the CAVs are allowed to ignore the traffic signs while exiting a traffic scenario when it is safe to do so.

In our simulation study, we consider high, medium and low traffic volumes for the test route as 500, 400 and 300 vehicles per hour, and for the adjacent roads as 800, 600 and 400 vehicles per hour, respectively.

B. Simulation Results and Analysis

We analyzed the implications of 11 different penetration rates of CAVs ranging from 0% to 100% that may have on fuel economy, travel time improvement as well as the mean speed changes and driving behavior. For the fuel consumption analysis, we used the polynomial metamodel presented in [40]. Using different penetration rates of CAVs, the simulation results allow several observations. First, for all traffic volumes, fuel economy increases when the penetration rate of CAVs increases, as shown in Fig. 2. From 0% to 40% penetration rates, the higher improvements are at low traffic volumes. Although in the optimal scenario (i.e., 100% CAVs), fuel economy improvement is between 24% and 33% at all traffic volumes, the improvement for 60% to 80% penetration rate is between 13% to 19%, with mean and standard deviation as shown in Table I. From a general fuel economy improvement point of view, the best CAV

penetration rate before the optimal scenario for all the traffic volumes is 70%, because it has the lowest standard deviation. Fuel economy improvement is increasing at all the traffic volumes as shown in Fig. 2. Similarly, the average travel time decreases, which represents an improvement in the network (Fig. 3). At low traffic volumes, the variations in average speed and travel time, represented by the blue lines in Fig. 3, are more gradual, in comparison with the other traffic volumes. High traffic volumes, represented by the yellow lines, have the most prominent changes, especially after 50% penetration. Medium traffic volumes, represented by the red lines, exhibit similar behavior but with some changes around 50% and 70% which we discussed more next.

TABLE I: Mean and standard deviation of fuel economy improvement of the three traffic volumes, from 60% to 80% penetration rate.

CAV penetration rate[%]	Mean	Standard Deviation
60%	13.83%	0.41
70%	16.12%	0.25
80%	17.89%	0.34

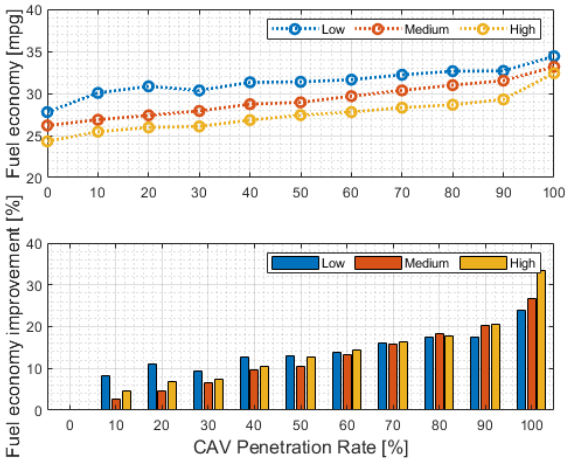

Fig. 2: Different penetration rates of CAVs impact on fuel economy, and fuel economy improvement. Both of them increases when the penetration increases, which represents improvement in the general network.

From a general view, the average travel time is decreasing for high and medium traffic volumes. In particular, the travel time distribution, illustrated in Fig. 4, shows how at a high traffic volume, all vehicles improve their travel times for a 50% penetration rate. At least 80% improve it by 5 s, which explains the strong change seen in Fig. 3 for that penetration rate. Since high traffic volume experiences more stop-and-go driving than the other traffic volumes, the 50% penetration rate of CAVs has an important impact on travel time decrement and average speed increment, as is going to be shown further in this section. At the low traffic

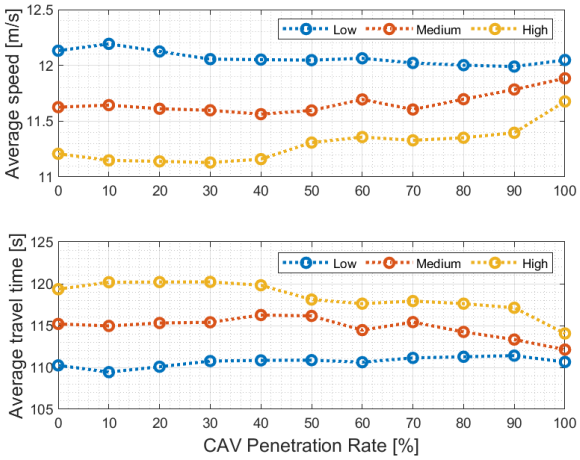

Fig. 3: Effect of different penetration rates of CAVs on average speed and travel time. Average speed increases while average travel time decreases for medium and high traffic volumes.

volume, the travel time distribution does not improve for 50% penetration rate, although at least 95% of the vehicles improve their travel times, as Fig. 4 illustrates. This is due to the fact that for this traffic volume, CAVs have an impact on fuel economy improvement, but not on average speed, as it is shown in Figs. 2 and 3. For a 50% penetration rate in medium traffic volume, at least 80% of the vehicles improve their times, but around 15% of them get worse times, which explains why average travel time increases for this penetration rate in Fig. 3. The same behavior is exhibited for the 70% penetration rate.

Considering the information presented in Figs. 3 and 4 at the high traffic volume, the average travel time improves for penetration rates above 50%, and has gradual changes for penetration rates from 10% to 40% and then again from 50% to 90%, as shown in Fig. 5. Although Figs. 3 and 5 present a decreasing slope for the high traffic volume, the remarkable improvements occur at 50% and 100% penetration rates. At a medium traffic volume, Fig. 3 shows that the average travel time is, in general, also decreasing, but the behavior is not the same. According to Fig. 5, the remarkable improvement for this traffic volume occurs at 60% and maintains a constant improvement after 70%. Considering the variations of average travel time, and consequently average speed for medium traffic volume at 70%, the best CAV penetration rate for this volume is 60%, and not 70% as was stated just with fuel consumption analysis.

Low traffic volume has its best performance at 10% penetration rate, and it remains slightly invariant up to 70%, where it gets worse. At 100%, the travel time variation is almost 0% compared to the baseline, which means that from this point of view, the best CAV penetration rate for low traffic volume is 10%. Consistently, Fig. 6 shows that, at the high traffic volume, travel time oscillates between 105 s and 155 s for all penetrations until 40%. For 50%, travel

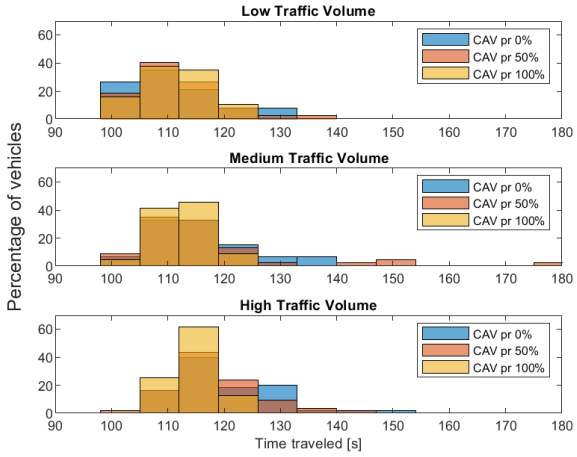

Fig. 4: Travel time distribution for each traffic volume at 0%, 50% and 100% CAV penetration rate. 50% illustrates how travel time distribution is changing, and its relationship with average travel time.

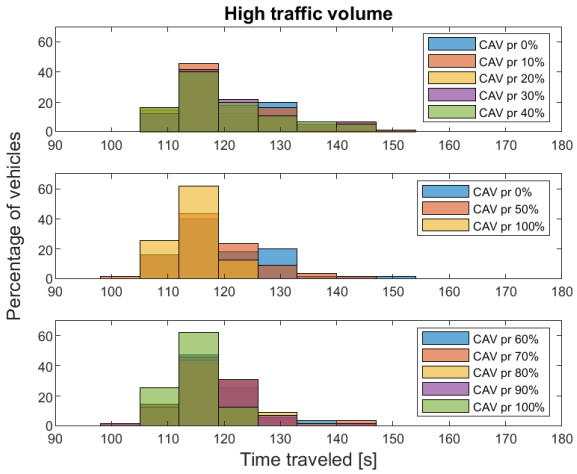

Fig. 6: Travel time distribution for high traffic volume at each penetration rate. A small variance is seen for penetration rates from 0% to 40%, and from 50% to 90%.

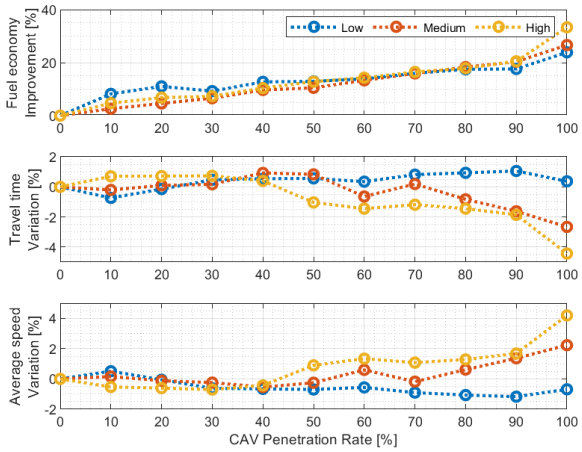

Fig. 5: Effect of partial penetration on percentage variation of fuel economy, travel time and average speed. 50% and 60% are interesting penetration rates for high traffic volume; 60% for medium, and 10 and 60% for low.

time goes from 98 s to 143 s, and it remains in that interval for all penetrations until 90%. Nevertheless, the travel time for penetrations from 50% to 90% is not the same, it keeps decreasing because, for each penetration rate, a higher number of vehicles get lower travel times. Correspondingly, Fig. 7 shows how travel time variation is decreasing for high traffic volume (represented by the yellow line), and average speed is increasing directly proportional to it, a combination that supports the fuel economy improvement seen in Fig.2.

Distribution for the medium traffic volume has its best improvements at 60% and 100% penetration rates. In particular with values between 98 s and 138 s for the first one, and 103 s and 121 s for the optimal scenario. The low traffic volume distribution is homogeneous, remaining between 95 s and 138 s for all penetrations. However, the distribution for 100% has values between 96 s and 121 s. Nevertheless, the behavior for medium traffic volume is different from high and low. For 50% penetration, more than 70% of the vehicles have travel times between 98 s and 119 s, but at least 8% of them have times from 140 s to 177 s, the highest travel time of the simulation. This 8% corresponds to HDVs and is responsible for the positive variation of travel time in Fig. 5.

Low traffic volume has an increasing average travel time, as shown in Fig. 3. Fig. 5 presents how CAVs penetration improves fuel economy by 9% for just 10% penetration, and it increases as the penetration rate increases. The travel time distribution in Fig. 7 illustrates why fuel economy is improving while travel time is not; this occurs when a greater portion of the vehicles share the same travel time, more than just somehow decreasing the average travel time. In other words, for this particular traffic volume, the travel time interval remains the same for at least 98% of the vehicles. The relationship between fuel economy improvement, travel time variation, and average speed variation is clearly illustrated in Fig. 5. At all traffic volumes, average speed variation is inversely proportional to travel time improvement. At the three traffic volumes, fuel economy improves as the penetration rate increases, even though at the low traffic volume the average speed is not increasing.

The variation of average speed profiles from high traffic volume is shown in Fig. 8, where the penetrations of interest are compared with the baseline and the optimal scenario. The critical penetrations at this volume are 50% and 60%. It is clear how the improvements of 35% and 40% happen between 200 m and 400 m, which corresponds to a portion of the first traffic scenario (i.e., on-ramp), and the part of the corridor immediately after it, and between 990 m and 1000

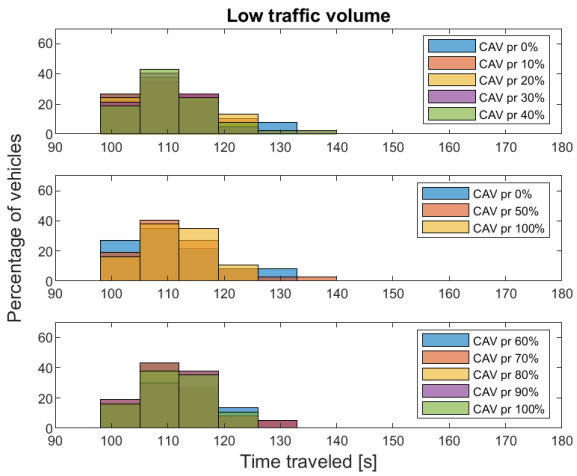

Fig. 7: Travel time distribution for low traffic volume at each penetration rate. Small variance is seen for all penetrations, but while penetration increases, more vehicles are sharing the same travel time.

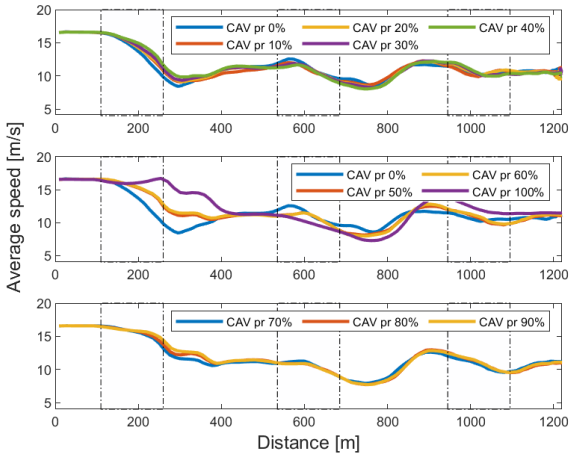

Fig. 8: High traffic volume average speed profile for each penetration rate, emphasizing in 50% and 60% as critical penetrations rates. Speed profile has gradual variations from 0% to 40%, and from 70% to 90%.

m, where the third traffic scenario (i.e., roundabout) occurs. It is also apparent how for penetrations smaller than 40%, the mean speed profile has small variations. The changes for 50% and 60% remain very close until 90% penetration.

Improvements in the speed profile are related to avoiding stop-and-go driving in conflict zones, like the first and the third traffic scenarios, and also with speed general reduction in zones like the second traffic scenario. The average speeds at the high traffic volume, shown in Figs. 8 and 9, correspond to the baseline case, 50% penetration case, and the optimal scenario case. Stop-and-go driving decreases while the penetration rate increases. The speed for the second traffic scenario decreases as well. The average speed in red

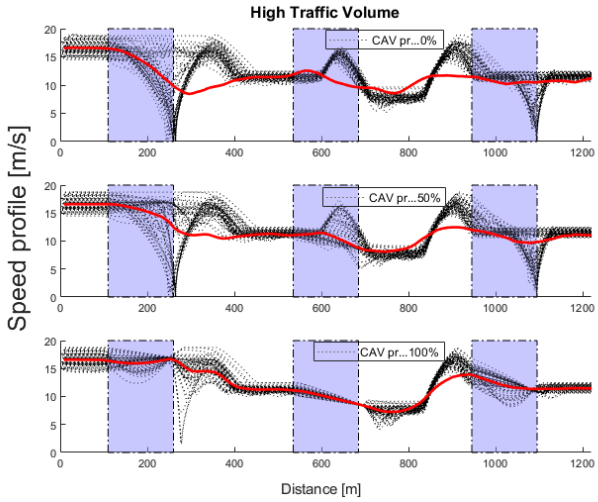

Fig. 9: High traffic volume speed profile at the baseline, critical penetration rate and optimal scenario. Stop-and-go driving decreases for 50% and is avoided for 100%.

becomes smoother while the speed profile of all the vehicles tends to converge to a single behavior, as happens in the optimal scenario.

C. Human-Driven Vehicles vs Connected and Automated Vehicles

The behavior of HDVs and CAVs differs from each other in mixed traffic scenarios as shown in Fig. 10 at the high traffic volume. The penetration rates of interest are 50% and 60%. In both cases, they are compared with the baseline and optimal scenario. Around the rates of interest, it can be seen that the CAVs dominate the speed profile improvement for the first and third traffic scenarios. However, the HDVs have better behavior in the speed reduction zone and a slight improvement near the end of the corridor. The performance improvement of the network for both penetrations of interest is due to the effect of CAVs and HDVs interaction. For 60% penetration rate at the medium traffic volume, the HDVs improve the average speed during the transitions before and after the third conflict zone (just along the last portion of the corridor) as it can be seen in Fig. 11. At the medium traffic volume, the improvement of the network is led by the CAVs. At the low traffic volume, CAVs and HDVs have similar behaviors for all the penetration rates of interest.

At all three traffic volumes, HDVs exhibit fuel economy improvement as it is shown in Table II. This is related to the information presented and discussed in Fig. 7. However, the best CAV penetration rate for the HDVs fuel economy is at 60% at all the traffic volumes. From Table II it can be stated that the best fuel economy improvement happens for 90%. However, for this penetration just 10% of the vehicles are HDVs, so the high percentage values reported on the table are not giving accurate information about an interesting improvement for HDVs fuel economy in a mixed traffic scenario.

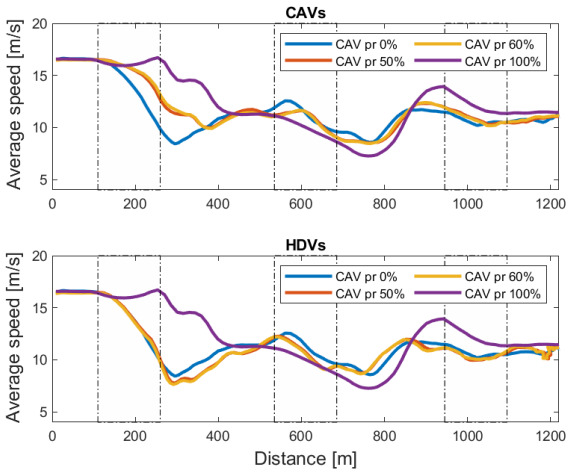

Fig. 10: High traffic volume average speed for CAVs and HDVs, in penetration rates of interest, compared with the baseline and optimal scenario.

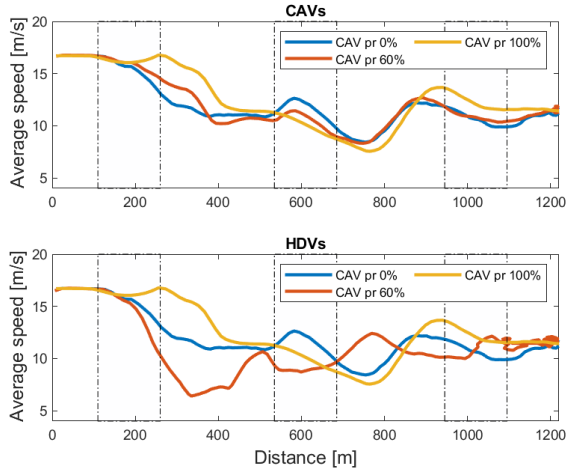

Fig. 11: Medium traffic volume average speed for CAVs and HDVs, in penetration rates of interest, compared with the baseline and optimal scenario.

V. Conclusion

In this paper, we developed a simulation framework to analyze the implications that different penetration rates of CAVs and their interaction with HDVs can have on fuel economy and travel time. We adopted the framework presented in [35] to capture the interaction between CAVs and HDVs. Using different penetration rates of CAVs, the results indicate that for low penetration rates fuel economy improvement is significant, although travel time and average speed do not improve. At this traffic volume, the best penetration rate for HDVs is 60%. At medium and high traffic volumes, we observed significant benefits in fuel economy while the penetration increases; however, the improvements in average speed and travel time have specific thresholds of interest, i.e., 60% penetration at the medium traffic volume, and 50% at the high traffic volume. The best penetration rate for HDVs is 60%.

TABLE II: Fuel economy improvement for HDVs. The best penetration rate for HDVs fuel economy improvement is 60% for the three traffic volumes.

CAV penetration rate [%]	Fuel economy improvement [%]		
	High	Medium	Low
10%	2.3%	-1%	0%
20%	0.3%	0.7%	5.4%
30%	-0.3%	1.7%	2.9%
40%	1.2%	-0.7%	3.1%
50%	2.7%	2%	4.1%
60%	2.6%	7.4%	7.2%
70%	0.5%	5.2%	9%
80%	-1.2%	7.5%	14.3%
90%	9.8%	18.7%	23.4%

It is expected that CAVs will gradually penetrate the market, interact with HDVs, and contend with vehicle-to-vehicle and vehicle-to-infrastructure communication limitations, e.g., bandwidth, dropouts, errors and/or delays. However, as we observed in this study, different penetration rates of CAVs can significantly alter transportation efficiency and safety. Ongoing work aims at optimally controlling the CAVs to indirectly control the HDVs and form platoons [41], [42]. A direction for future research should synergistically integrate human-driving behavior, control theory, and learning in an effort to develop a framework to address a fundamental gab on current methods for safe co-existence of CAVs with HDVs. The framework will aim CAVs at coordinating with HDVs safely at any traffic scenario, e.g., crossing signal-free intersections, merging at roadways and roundabouts, cruising in congested traffic, passing through speed reduction zones, and lane- merging or passing maneuvers. Ongoing.

References

[1] R. Margiotta and D. Snyder, "An agency guide on how to establish localized congestion mitigation programs," U.S. Department of Transportation. Federal Highway Administration, Tech. Rep., 2011.

[2] J. Lee, B. B. Park, K. Malakorn, and J. J. So, "Sustainability assessments of cooperative vehicle intersection control at an urban corridor," *Transportation Research Part C: Emerging Technologies*, vol. 32, pp. 193–206, 2013.

[3] B. Chalaki and A. A. Malikopoulos, "Time-optimal coordination for connected and automated vehicles at adjacent intersections," *IEEE Transactions on Intelligent Transportation Systems*, pp. 1–16, 2021.

[4] C. Letter and L. Elefteriadou, "Efficient control of fully automated connected vehicles at freeway merge segments," *Transportation Research Part C: Emerging Technologies*, vol. 80, pp. 190–205, 2017.

[5] A. Mosebach, S. Röchner, and J. Lunze, "Merging control of cooperative vehicles," *IFAC-PapersOnLine*, vol. 49, no. 11, pp. 168–174, 2016.

[6] J. Guanetti, Y. Kim, and F. Borrelli, "Control of Connected and Automated Vehicles: State of the Art and Future Challenges," *Annual Reviews in Control*, vol. 45, pp. 18–40, 2018.

[7] A. de La Fortelle, "Analysis of reservation algorithms for cooperative planning at intersections," *13th International IEEE Conference on Intelligent Transportation Systems*, pp. 445–449, Sep. 2010.

[8] K. Dresner and P. Stone, "A multiagent approach to autonomous intersection management," *Journal of artificial intelligence research*, vol. 31, pp. 591–656, 2008.

[9] S. E. Shladover, C. A. Desoer, J. K. Hedrick, M. Tomizuka, J. Walrand, W.-B. Zhang, D. H. McMahon, H. Peng, S. Sheikholeslam, and N. McKeown, "Automated vehicle control developments in the PATH program," *IEEE Transactions on Vehicular Technology*, vol. 40, no. 1, pp. 114–130, 1991.

[10] V. Milanes, J. Villagra, J. Godoy, J. Simo, J. Perez, and E. Onieva, "An Intelligent V2I-Based Traffic Management System," pp. 49–58, 2012.

[11] I. A. Ntousakis, I. K. Nikolos, and M. Papageorgiou, "Optimal vehicle trajectory planning in the context of cooperative merging on highways," *Transportation Research Part C: Emerging Technologies*, vol. 71, pp. 464–488, 2016.

[12] A. Bakibillah, M. Kamal, C. Tan *et al.*, "The optimal coordination of connected and automated vehicles at roundabouts," in *2019 58th Annual Conference of the Society of Instrument and Control Engineers of Japan (SICE)*. IEEE, 2019, pp. 1392–1397.

[13] A. I. Mahbub, A. A. Malikopoulos, and L. Zhao, "Decentralized optimal coordination of connected and automated vehicles for multiple traffic scenarios," *Automatica*, vol. 117, no. 108958, 2020.

[14] A. M. I. Mahbub, A. A. Malikopoulos, and L. Zhao, "Impact of connected and automated vehicles in a corridor," in *Proceedings of 2020 American Control Conference, 2020*. IEEE, 2020, pp. 1185–1190.

[15] A. Kotsialos and M. Papageorgiou, "Nonlinear optimal control applied to coordinated ramp metering," *IEEE Transactions on control systems technology*, vol. 12, no. 6, pp. 920–933, 2004.

[16] S. Kumaravel, A. A. Malikopoulos, and R. Ayyagari, "Optimal coordination of platoons of connected and automated vehicles at signal-free intersections," *IEEE Transactions on Intelligent Vehicles*, pp. 1–1, 2021.

[17] A. Alessandrini, A. Campagna, P. Delle Site, F. Filippi, and L. Persia, "Automated vehicles and the rethinking of mobility and cities," *Transportation Research Procedia*, vol. 5, pp. 145–160, 2015.

[18] Y. Zheng, S. E. Li, K. Li, and W. Ren, "Platooning of connected vehicles with undirected topologies: Robustness analysis and distributed h-infinity controller synthesis," *IEEE Transactions on Intelligent Transportation Systems*, vol. 19, no. 5, pp. 1353–1364, 2017.

[19] G. Sharon and P. Stone, "A protocol for mixed autonomous and human-operated vehicles at intersections," in *International Conference on Autonomous Agents and Multiagent Systems*. Springer, 2017, pp. 151–167.

[20] V. Milanés, S. E. Shladover, J. Spring, C. Nowakowski, H. Kawazoe, and M. Nakamura, "Cooperative adaptive cruise control in real traffic situations," *IEEE Transactions on intelligent transportation systems*, vol. 15, no. 1, pp. 296–305, 2013.

[21] I. G. Jin, G. Orosz, D. Hajdu, T. Insperger, and J. Moehlis, "To delay or not to delay—stability of connected cruise control," in *Time Delay Systems*. Springer, 2017, pp. 263–282.

[22] D. Hajdu, I. G. Jin, T. Insperger, and G. Orosz, "Robust design of connected cruise control among human-driven vehicles," *IEEE Transactions on Intelligent Transportation Systems*, vol. 21, no. 2, pp. 749–761, 2019.

[23] G. Orosz, "Connected cruise control: modelling, delay effects, and nonlinear behaviour," *Vehicle System Dynamics*, vol. 54, no. 8, pp. 1147–1176, 2016.

[24] S. I. Guler, M. Menendez, and L. Meier, "Using connected vehicle technology to improve the efficiency of intersections," *Transportation Research Part C: Emerging Technologies*, vol. 46, pp. 121–131, 2014.

[25] P. Gipps, "A behavioural car-following model for computer simulation," *Transportation Research Part B: Methodological*, vol. 15, no. 2, pp. 105–111, 1981.

[26] R. Wiedemann, "Simulation des strassenverkehrsflusses." 1974.

[27] Y. Zhang and C. G. Cassandras, "The penetration effect of connected automated vehicles in urban traffic: an energy impact study," in *2018 ieee conference on control technology and applications (ccta)*. IEEE, 2018, pp. 620–625.

[28] J. Ding, H. Peng, Y. Zhang, and L. Li, "Penetration effect of connected and automated vehicles on cooperative on-ramp merging," *IET Intelligent Transport Systems*, vol. 14, no. 1, pp. 56–64, 2020.

[29] N. Wan, A. Vahidi, and A. Luckow, "Optimal speed advisory for connected vehicles in arterial roads and the impact on mixed traffic," *Transportation Research Part C: Emerging Technologies*, vol. 69, pp. 548–563, 2016.

[30] A. R. Kreidieh, C. Wu, and A. M. Bayen, "Dissipating stop-and-go waves in closed and open networks via deep reinforcement learning," in *2018 21st International Conference on Intelligent Transportation Systems (ITSC)*. IEEE, 2018, pp. 1475–1480.

[31] C. Wu, K. Parvate, N. Kheterpal, L. Dickstein, A. Mehta, E. Vinitsky, and A. M. Bayen, "Framework for control and deep reinforcement learning in traffic," in *2017 IEEE 20th International Conference on Intelligent Transportation Systems (ITSC)*. IEEE, 2017, pp. 1–8.

[32] B. Ran, S. Leight, and B. Chang, "A microscopic simulation model for merging control on a dedicated-lane automated highway system," *Transportation Research Part C: Emerging Technologies*, vol. 7, no. 6, pp. 369–388, 1999.

[33] K. Li and P. Ioannou, "Modeling of traffic flow of automated vehicles," *IEEE Transactions on Intelligent Transportation Systems*, vol. 5, no. 2, pp. 99–113, 2004.

[34] T. Taleb, E. Sakhaee, A. Jamalipour, K. Hashimoto, N. Kato, and Y. Nemoto, "A Stable Routing Protocol to Support ITS Services in VANET Networks," pp. 3337–3347, 2007.

[35] A. M. I. Mahbub, V. Karri, D. Parikh, S. Jade, and A. A. Malikopoulos, "A decentralized time- and energy-optimal control framework for connected automated vehicles: From simulation to field test," in *SAE Technical Paper 2020-01-0579*. SAE International, 2020.

[36] A. E. Bryson and Y. C. Ho, *Applied optimal control: optimization, estimation and control*. CRC Press, 1975.

[37] A. M. I. Mahbub and A. A. Malikopoulos, "Conditions to Provable System-Wide Optimal Coordination of Connected and Automated Vehicles," *Automatica*, vol. 131, no. 109751, 2021.

[38] P. Group *et al.*, "Ptv vissim 7 user manual," *Germany: PTV GROUP*, 2014.

[39] M. Fellendorf and P. Vortisch, "Microscopic traffic flow simulator vissim," in *Fundamentals of traffic simulation*. Springer, 2010, pp. 63–93.

[40] M. Kamal, M. Mukai, J. Murata, and T. Kawabe, "Model Predictive Control of Vehicles on Urban Roads for Improved Fuel Economy," *IEEE Transactions on Control Systems Technology*, vol. 21, no. 3, pp. 831–841, 2013.

[41] A. M. I. Mahbub and A. A. Malikopoulos, "A Platoon Formation Framework in a Mixed Traffic Environment," *IEEE Control Systems Letters (LCSS)*, vol. 6, pp. 1370–1375, 2021.

[42] A. M. Ishtiaque Mahbub and A. A. Malikopoulos, "Platoon Formation in a Mixed Traffic Environment: A Model-Agnostic Optimal Control Approach," *Proceedings of 2022 American Control Conference*, Oct. 2022 (to appear).